Research Article

Journal of Molecular Recognition

Received: 28 May 2010, Revised: 19 October 2010, Accepted: 20 October 2010, Published online in Wiley Online Library: 2011

(wileyonlinelibrary.com) DOI:10.1002/jmr.1113

Effect of the beta-sheet-breaker peptide LPFFD on oriented network of amyloid β25-35 fibrils†

Ünige Murvai[a], Katalin Soós[b], Botond Penke[c] and Miklós S. Z. Kellermayer[a]*

Amyloid fibrils are self-associating filamentous structures deposited in extracellular tissue in various neurodegenerative and protein misfolding disorders. It has been shown that beta-sheet-breaker (BSB) peptides may interfere with amyloid fibril assembly. Although BSB peptides are prospective therapeutic agents in amyloidosis, there is ambiguity about the mechanisms and generality of their action. In the present work we analyzed the effect of the BSB peptide LPFFD on the growth kinetics, morphologic, and mechanical properties of amyloid β25-35 (Aβ25-35) fibrils assembled in an oriented array on mica surface. Aβ25-35 is thought to represent the biologically active, toxic fragment of the full-length Aβ peptide. Growth kinetics and morphologic features were analyzed using *in situ* atomic force microscopy in the presence of various concentrations of LPFFD. We found that the addition of LPFFD only slightly altered the assembly kinetics of Aβ25-35 fibrils. Already formed fibrils did not disassemble in the presence of high concentrations of LPFFD. The mechanical stability of the fibrils was explored with force spectroscopy methods. The nanomechanical behavior of Aβ25-35 fibrils is characterized by the appearance of force staircases which correspond to the force-driven unzipping and dissociation of several protofilaments. In the presence of LPFFD single-plateau force traces dominated. The effects of LPFFD on Aβ25-35 fibril assembly and stability suggest that inter-protofilament interactions were slightly weakened. Complete disassembly of fibrils, however, was not observed. Thus, under the conditions explored here, LPFFD may not be considered as a BSB peptide with generalized beta-sheet breaking properties. Copyright © 2011 John Wiley & Sons, Ltd.

Keywords: atomic force microscopy; beta-amyloid; beta-sheet breaker peptide

INTRODUCTION

Amyloid fibrils are filamentous aggregates which can be found in extracellular tissue-deposits in various degenerative disorders (Selkoe, 1997, 2001; Serpell *et al*., 2000; Hardy and Selkoe, 2002). The full-length (39- to 43-residue-long) amyloid β (Aβ) peptide is the major component of neuritic plaques found in Alzheimer's disease (Selkoe, 1997). Aβ forms self-associating fibrillar structures possessing predominantly cross-β conformation (Serpell *et al*., 2000).

The amyloid β 25-35 peptide (Aβ25-35) is an eleven-residue-long fragment of the full-length Aβ. It is a fibril-forming peptide that represents the biologically active, toxic form of the full-length Aβ monomer (Yankner *et al*., 1990; Forloni *et al*., 1993).

LPFFD (Lys-Pro-Phe-Phe-Asp) is a five-residue-long beta-sheet-breaker (BSB) peptide, also called as Soto's pentapeptide. BSB peptides are rationally designed peptides specially created to break β-sheets. Formation of misfolded Aβ involves the organization of several Aβ monomers in an oligomeric β-sheet structure stabilized by hydrogen bonds and hydrophobic interactions. β-sheet-breaker peptides contain a sequence similar to the region involved in protein–protein interactions (the self-recognition motif) but also include some residues unable to fit inside a β-sheet structure. β-sheet-breaker peptides may destabilize the misfolded Aβ oligomers, and consequently prevent amyloid formation (Soto *et al*., 1998). Even though the mechanism by which β-sheet-breaker peptides inhibit and reverse fibril formation has not yet been identified, two distinct molecular events are thought to be important. First, binding between β-sheet-breaker peptides and Aβ and second, conformational destabilization of β-sheet structures (Estrada and Soto, 2007).

To investigate whether the LPFFD possesses generalized beta-sheet-breaking properties, we have tested these two molecular events (assembly and disassembly) on Aβ25-35

* *Correspondence to: M. S. Z. Kellermayer, Department of Biophysics and Radiation Biology, Semmelweis University, Tűzoltó u. 37-47, Budapest H-1094, Hungary.*
E-mail: miklos.kellermayer@eok.sote.hu

a *Ü. Murvai, M. S. Z. Kellermayer*
Department of Biophysics and Radiation Biology, Semmelweis University, Tűzoltó u. 37-47, Budapest H-1094, Hungary

b *K. Soós*
Department of Medical Chemistry, University of Szeged, Dóm tér 8., Szeged H-6720, Hungary

c *B. Penke*
Supramolecular and Nanostructured Materials Research Group of the Hungarian Academy of Sciences, Dóm tér 8., Szeged H-6720, Hungary

† *This article is published in Journal of Molecular Recognition as a focus on AFM on Life Sciences and Medicine, edited by Jean-Luc Pellequer and Pierre Parot (CEA Marcoule, Life Science Division, Bagnols sur Cèze, France).*

peptides. Using Aβ25-35 fibrils as a model system provides several advantages. Aβ25-35 fibrils display a highly ordered trigonal arrangement on the freshly cleaved mica surface (Karsai *et al*., 2007). The stable, ordered network of Aβ25-35 fibrils on mica is a simple, reproducible system on the nanoscale. Studying the effect of BSB peptides on this model, the changes of structural, nanomechanical properties of the Aβ25-35 fibril network can be easily monitored by atomic force microscopy (AFM).

In the present work, we explored the effect of LPFFD on the growth, orientation, and force spectra of the Aβ25-35 fibrils epitaxially grown on mica. We find that LPFFD, even at high concentrations, did not significantly influence the global structural features, assembly dynamics, and stability of Aβ25-35 fibrils.

MATERIALS AND METHODS

Sample preparation

Lyophilized samples Aβ25-35 (^{25}GSNKGAIIGLM^{35}-amide) peptide produced by solid state synthesis (Zarandi *et al*., 2007) were dissolved in DMSO (dimethyl sulfoxide) and transferred to Na-phosphate buffer ["Na-PBSA," 10 mM Na-phosphate (pH 7.4), 140 mM NaCl, 0.02% NaN_3] at a final concentration of 2–2.5 mg/ml. To remove oligomeric aggregates the solution was centrifuged with 250,000*g* at 4°C for 2 h (Beckman Coulter Optima^{TM} MAX Ultracentrifuge). The supernatant was diluted for further use. Peptide concentration was measured with the quantitative bicinchoninic acid assay (Smith *et al*., 1985).

The BSB peptide LPFFD, also called as Soto's pentapeptide (Soto *et al*., 1998), was produced by solid state synthesis. Lyophilized samples were dissolved in Na-PBSA at final concentration of 1.5–1.8 mM.

Atomic force microscopy

Typically 100 μl samples were applied to a freshly cleaved mica surface. We used high-grade mica sheets (V2 grade, #52-6, Ted Pella, Inc., Redding, CA). After incubating the sample for 10 min the surface was washed gently with Na-PBSA buffer to remove unbound fibrils. The samples were imaged with AFM in buffer. Non-contact mode AFM images were acquired with an Asylum Research MFP3D instrument (Santa Barbara, CA) using silicon-nitride cantilevers (Olympus BioLever, resonance frequency in buffer ~9 kHz). 512 × 512-pixel images were collected at a typical scanning frequency of 0.8–1.5 Hz and with a high set point (0.8–1 V).

In situ AFM

Time-lapse AFM images of Aβ25-35 fibril growth on mica were recorded by repetitively scanning 2 μm wide areas following the addition of the peptides. 512 × 512 pixel images were typically scanned at a rate of 2 Hz. Usually at least ten images were collected with no interleave pause. In control experiments a 100-μl Aβ25-35 solution (8 μM) was pipetted onto a freshly cleaved mica surface, then the recording of time-lapse AFM images was immediately started. For studying the effect of the LPFFD peptide on Aβ25-35 fibril assembly kinetics, a 100-μl sample of Aβ25-35/LPFFD mixture (8 μM Aβ25-35, 300 μM LPFFD) was applied to the freshly cleaved mica surface, and time-lapse AFM images were immediately recorded.

Force spectroscopy

Force spectroscopy measurements were carried out according to procedures published before (Kellermayer *et al*., 2005; Karsai *et al*., 2006b). Briefly, surface-bound fibrils were mechanically manipulated by first pressing the cantilever (Olympus BioLever, lever A) tip against the surface, then pulling the cantilever away with a constant, pre-adjusted rate. Typical stretch rate was 500 nm/s. Experiments were carried out under aqueous buffer conditions (Na-PBS buffer, pH 7.4). Stiffness was determined for each cantilever by using the thermal method (Hutter and Bechhoefer, 1993). To explore the effect of LPFFD on the nanomechanical behavior of Aβ25-35, the fibrils were manipulated in the presence of the BSB peptide. A 100-μl sample of Aβ25-35/LPFFD mixture (8 μM Aβ25-35 and 196 μM LPFFD) was pipetted on freshly cleaved mica, then allowed to incubate for

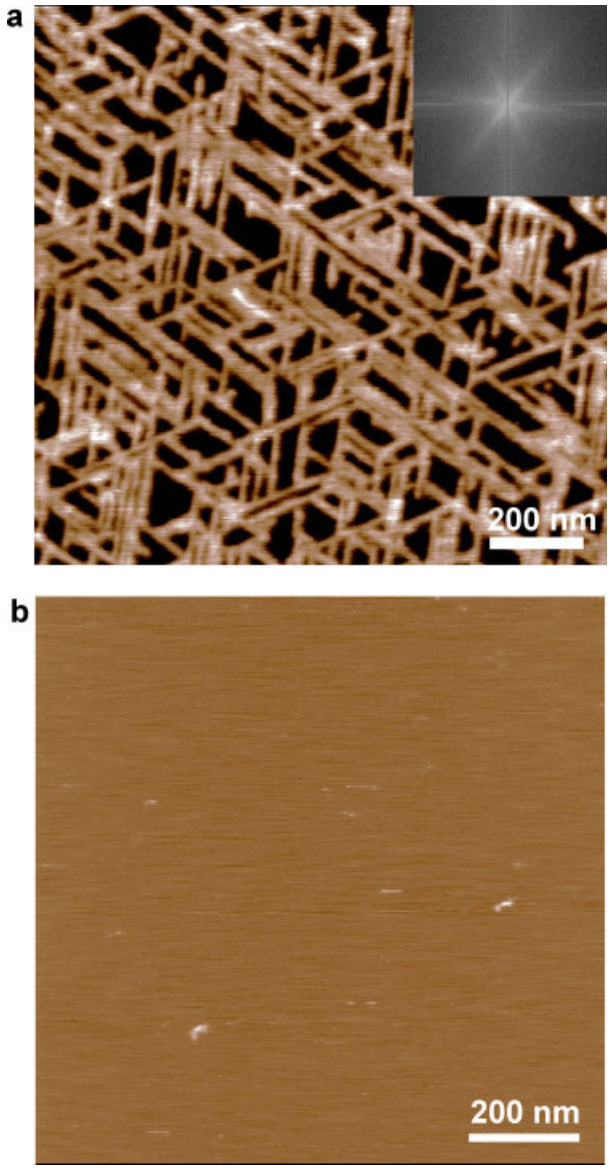

Figure 1. AFM images of control specimens. (a) AFM image of oriented Aβ25-35 fibril network on mica surface. Inset: 2D-FFT of AFM image. (b) AFM image of mica surface following the incubation of a 1 mM solution of LPFFD for 45 min.

Journal of Molecular Recognition

90 min. Unbound fibrils were removed by washing gently with Na-PBSA buffer. Aβ25-35 fibrils without LPFFD served as control.

Image processing and data analysis

AFM images and force spectra were analyzed using built-in algorithms of the IgorPro v6.03 MFP3D controller software (Wavemetrics, Lake Oswego, OR). Orientation angles of fibrils were measured manually between a line fitted to the fibril axis and a horizontal reference line. 2D FFT was carried out with ImageJ software (public domain). For data analysis, we used IgorPro v6.0 and KaleidaGraph 4.0 software packages.

RESULTS

Control experiments

The oriented network of Aβ25-35 fibrils grown epitaxially on mica was used in the present work as a model system for rapid amyloid fibril assembly. Figure 1a shows this oriented network model used as control. The fibrils are highly oriented with an angle of 60° between individual fibrils, and 120° between each of the three main orientation directions. These three directions are represented in a regular hexagonal pattern on the 2D FFT image (Figure 1a inset). The fibrils have reached lengths so that they touch each other; therefore, very few free fibril ends are observed. Depending on the initial peptide concentration the oriented Aβ25-35 network forms with different rates on the time scale of minutes to hours. Because of the accelerated fibrillogenesis, the effect of physical and chemical parameters on amyloid fibrillogenesis can be easily explored. The effect of the LPFFD peptide was investigated on various parameters of the structure and formation of the oriented Aβ25-35 network.

To test whether the LPFFD peptide itself forms fibrils on the mica surface, a 1 mM LPFFD solution was incubated on freshly cleaved mica for 45 min at room temperature. After washing the surface with buffer to remove the excess LPFFD solution, we scanned the surface with AFM (Figure 1b). The AFM image shows a mica

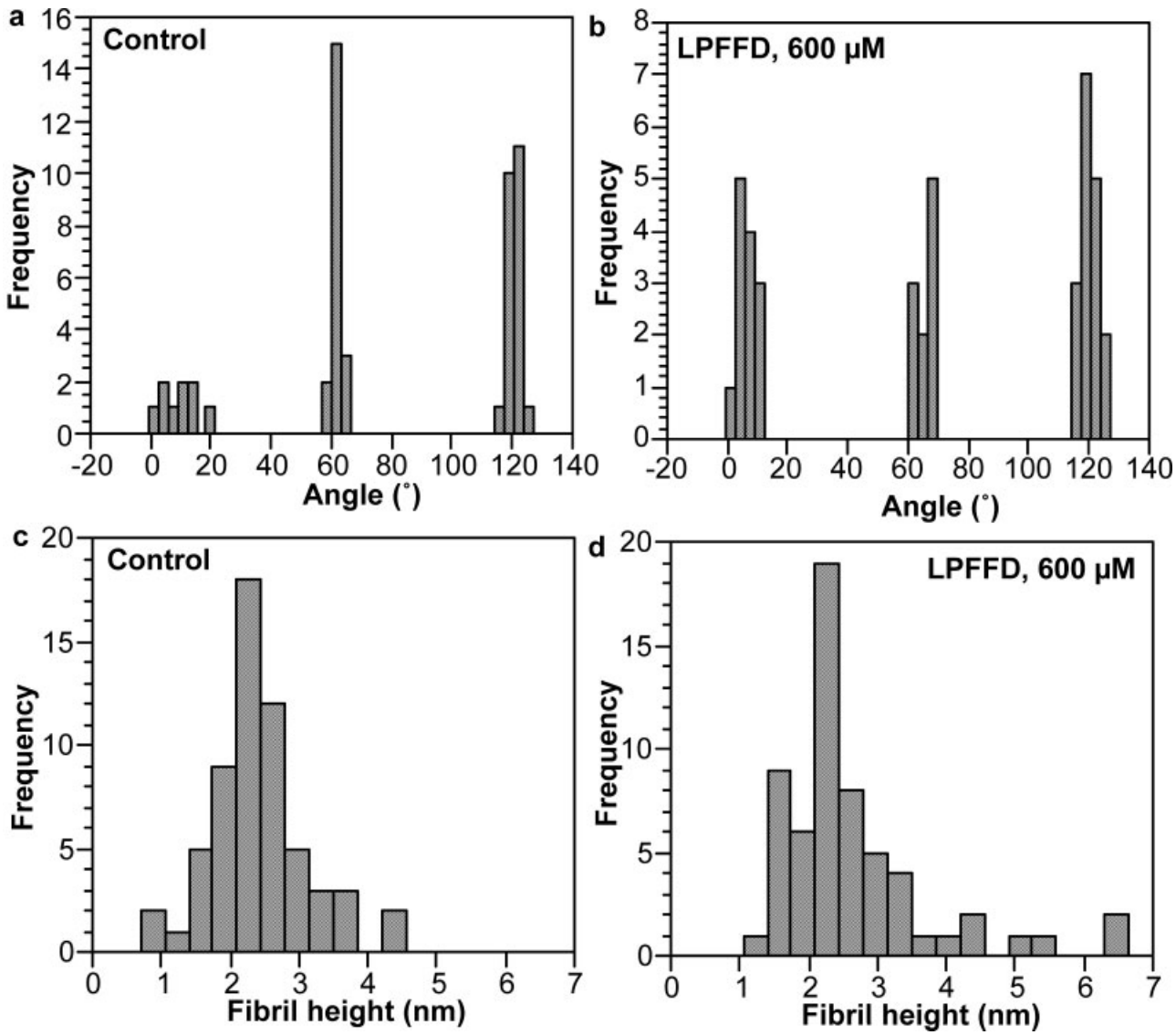

Figure 2. Angle-distribution of oriented Aβ25-35 fibrils (8 μM) on mica in the absence (a) and presence (b) of LPFFD peptides (600 μM). Topographical height-distribution of oriented Aβ25-35 fibrils (8 μM) on mica in the absence (c) and presence (d) of LPFFD peptides (600 μM).

surface devoid of filamentous structures. Thus, the LPFFD peptide by itself did not form aggregates or fibrils on the mica surface.

Effect of LPFFD on the orientation, structure, and assembly dynamics of A*β*25-35 fibrils on mica

To investigate the effect of LPFFD on the global structure of the Aβ25-35 network, we first measured the fibril orientation angles in LPFFD-treated samples. Figure 2 shows the results. The orientation angles in the control sample (Figure 2a) were narrowly distributed around 0, 60, and 120°, thus revealing discrete, 60° differences between fibril orientations. The orientation angles of fibrils formed in the presence of 600 μM LPFFD display a similar distribution (Figure 2b).

The overall structural features of Aβ25-35 fibrils were assessed by measuring their topographical height in the absence and presence of LPFFD. The height distributions of control and LPFFD-treated fibrils are shown in Figure 2c and d, respectively. The mean fibril height was 2.41 nm (±0.09 nm SEM, $n = 60$) and 2.64 nm (±0.14 nm SEM, $n = 60$) for the control and

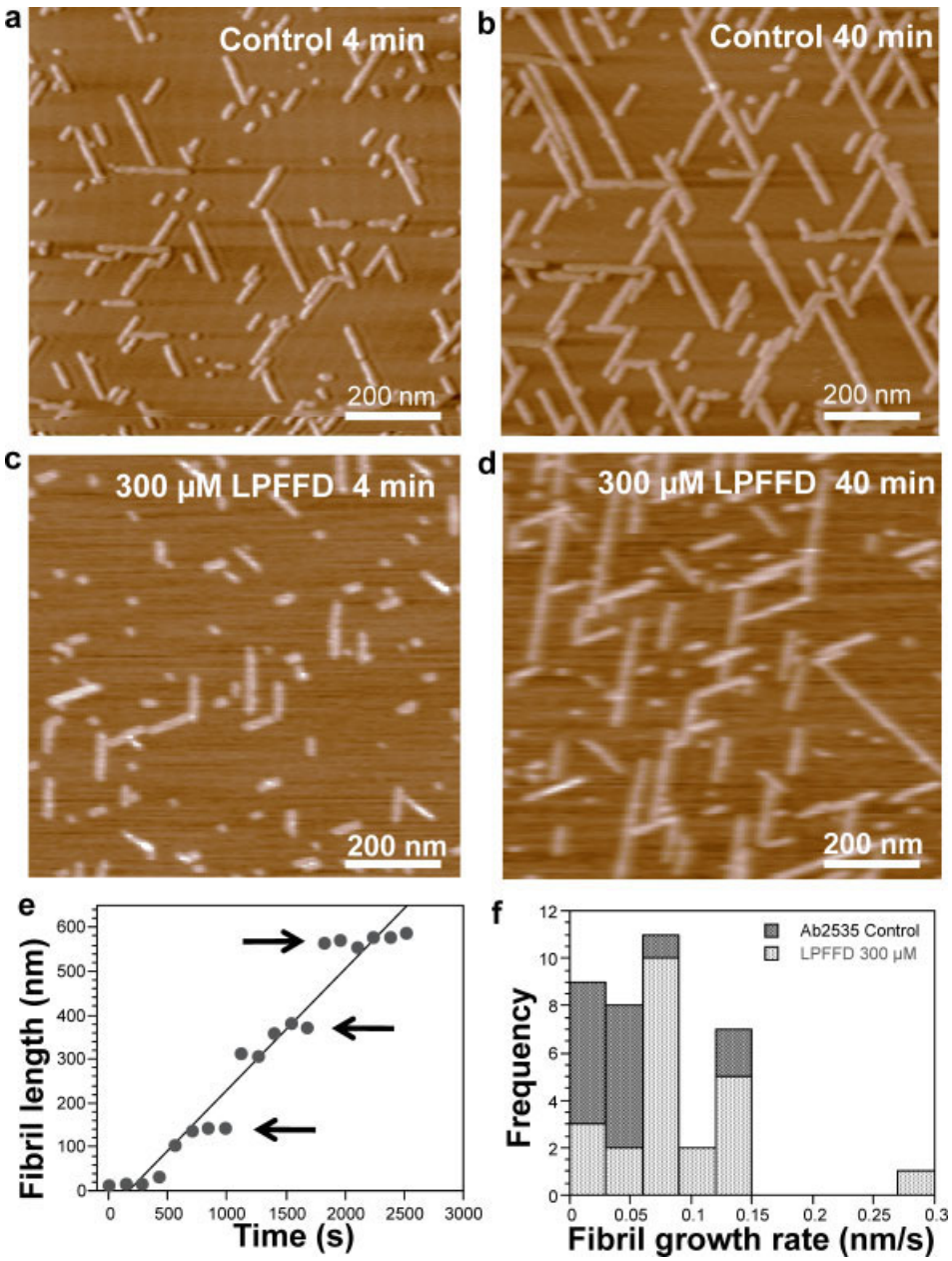

Figure 3. Effect of LPFFD on the growth rate of Aβ25-35 fibrils. (a) and (b) are the first and last images, respectively, of the control sample during an *in situ* AFM experiment. The oriented network of Aβ25-35 was formed at a peptide concentration of 8 μM. (c) and (d) are the first and last images, respectively, of the LPFFD-treated sample during an *in situ* AFM experiment. The fibril network, formed at an Aβ25-35 peptide concentration of 8 μM, was allowed to grow in the presence of 300 μM LPFFD. (e) Increase of Aβ25-35 fibril length as a function of time. Arrows point at periods of pauses during fibril growth. The fibril length versus time data were fitted with linear function so as to obtain average fibril growth rate from the slope. (f) Distribution of fibril growth rate for control (dark gray) and LPFFD-treated (light gray) samples.

Journal of Molecular Recognition

LPFFD-treated samples, respectively. There was no significant difference between the mean fibril heights (*t* probability 0.2).

The effect of LPFFD on the kinetics of Aβ25-35 fibril growth was investigated by monitoring the length of individual fibrils as a function of time in the presence of LPFFD during time-lapse *in situ* AFM experiments (Figure 3). A 100 μl sample from a mixture of 300 μM LPFFD and 8 μM Aβ25-35 was applied to the freshly cleaved mica surface, then AFM images were continuously recorded of the same sample surface. The acquisition of an image took 100 s. The evolution of fibrillar network during the examined time period was similar in the case of the control (Figure 3a and b) and LPFFD-treated (Figure 3c and d) samples. The growth of individual fibrils could be captured in both cases. Fibrils grew until they reached another fibril lying across their growth path. The instantaneous length of a single fibril as a function of time is shown in Figure 3e. Although steps and pauses can be discerned in the trace (arrows) the average growth can be fitted with a linear function. Figure 3f shows the distribution of fibril velocities for control and LPFFD-treated samples across the range of 0.3 nm/s. The mean fibril growth rates were 0.16 nm/s (±0.08 nm/s SEM, $n = 17$) and 0.08 nm/s (±0.01 nm/s SEM, $n = 23$) for the control and LPFFD-treated samples, respectively. Given the deviation from normal distribution we compared the fibril growth rates with the non-parametric Mann–Whitney test, which showed that there are no significant differences between them.

Effect of LPFFD on the disassembly of A*β*25-35 fibrils *in vitro*

The fibril dismantling effect (Sigurdsson *et al*., 2000) of the LPFFD peptide was investigated by treating a mature Aβ25-35 fibril network with large concentrations of LPFFD (Figure 4). First a dense, oriented amyloid network was generated (Figure 4a), then the surface was washed gently with PBSA buffer to remove the unbound fibrils, and finally the network was incubated in the presence of 1.58 mM LPFFD solution at room temperature for 80 min (Figure 4b). The relative surface coverage was calculated. Although a 10% decrease in surface coverage is evoked by the addition of LPFFD, similar effects are achieved by washing the surface with buffer solution.

Effect of LPFFD on the nanomechanics of A*β*25-35 fibrils

The effect of LPFFD on the mechanical stability of oriented Aβ25-35 fibrils was explored by manipulating the fibrils in the presence of the peptide. The nanomechanical behavior of Aβ25-35 fibrils is characterized by the appearance of force plateaus which correspond to the force-driven unzipping of protofilaments (Figure 5a top). In the presence of 196 μM LPFFD the global appearance of the force curves was similar to that of the control, but the number of force steps was reduced, and longer force plateaus could be observed (Figure 5a bottom). The distribution of plateau lengths for the control and LPFFD-treated samples is shown in Figure 5b. In the presence of LPFFD a wider distribution of plateau lengths is observed, with lengths up to 220 nm. Figure 5c shows the distribution of plateau forces for the control and LPFFD-treated samples. Whereas a multimodal distribution is clearly seen in the control, the plateau forces in the LPFFD-treated sample are distributed relatively narrowly around a single maximum at ~60 pN.

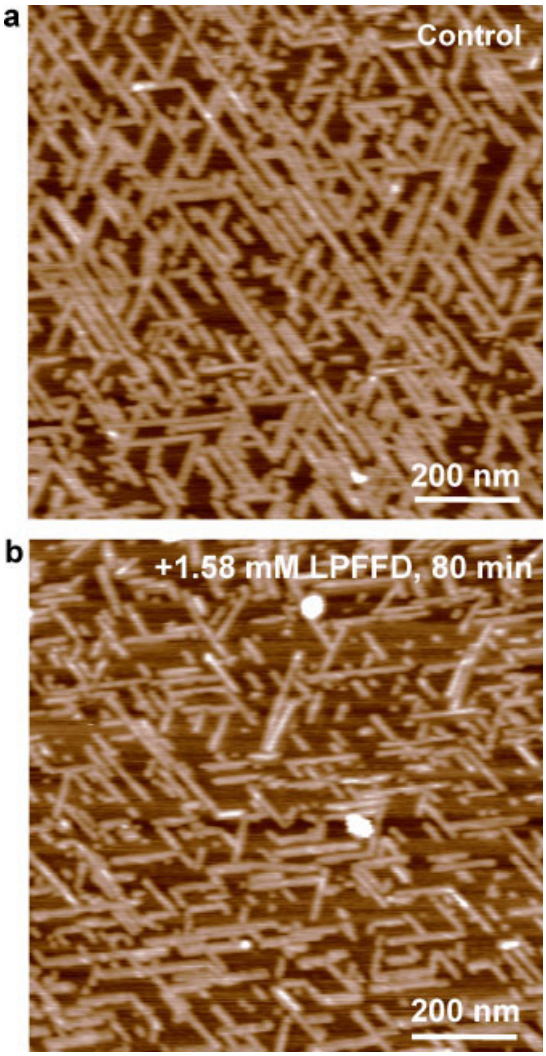

Figure 4. Effect of LPFFD on the stability of already existing Aβ25-35 network. (a) Control sample. (b) Aβ25-35 network treated with 1.58 mM LPFFD for 80 min.

DISCUSSION

We have recently shown that the Aβ25-35 peptide, which is thought to represent the toxic fragment of the full-length amyloid beta-peptide (Yankner *et al*., 1990; Forloni *et al*., 1993), and its mutant form (Aβ25-35_N27C) forms a highly oriented network on the surface of mica (Karsai *et al*., 2007, 2008; Kellermayer *et al*., 2008). The growth of the fibrils is epitaxially driven and occurs on a time scale significantly shorter than in bulk solution (Kellermayer *et al*., 2008). The rapid formation of fibrils, and the possibilities of parameterizing global and local fibril structure as well as following the kinetics of individual fibril growth make the oriented Aβ25-35 fibril network an appealing experimental model system. In the present work we investigated the effect of the LPFFD beta-sheet-breaking (BSB) peptide (Soto *et al*., 1998) on the structure, dynamics, and nanomechanics of the oriented Aβ25-35 fibril network. Although BSB peptides are designed according to targeted amyloid peptide sequences (Tjernberg *et al*., 1996, 1999; Soto *et al*., 1998; Estrada and Soto, 2007), they are expected to possess generalized beta-sheet disrupting properties, particularly because amyloid fibrils are held together primarily by peptide backbone interactions

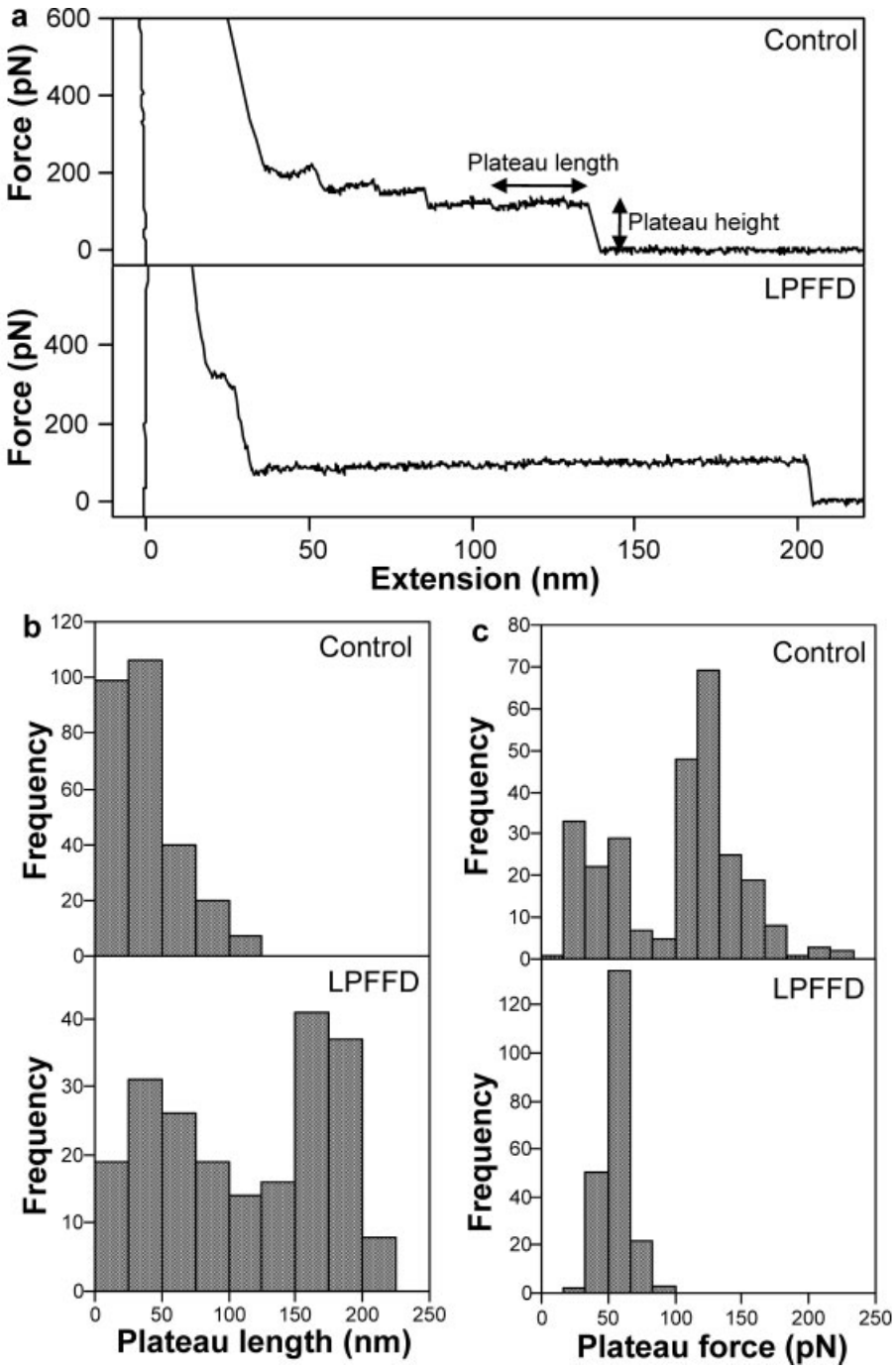

Figure 5. Effect of LPFFD on the force spectra of epitaxially grown Aβ25-35 fibrils. (a) Examples of force curves control (top) and LPFFD-treated (196 μM, bottom) samples. Only the cantilever retraction data are shown. (b) Distribution of plateau length for control (top) and LPFFD-treated (bottom) samples. (c) Distribution of plateau force for control (top) and LPFFD-treated (bottom) samples.

(Tycko, 2004). Thus, the investigation of the effect of such peptides in our experimental model system is well warranted. LPFFD (Lys-Pro-Phe-Phe-Asp) is a five-residue long BSB peptide designed towards the hydrophobic core region (residues 17-21) of the full-length Aβ1-40 peptide (Soto *et al.*, 1998). Although the targeted sequence is not present in Aβ25-35, based on the generalized BSB effect LPFFD may in principle influence the global appearance and assembly/disassembly dynamics of Aβ25-35 fibrils.

We find in numerous experiments that the global structural features, assembly-dynamics, and stability of the Aβ25-35 network are not influenced significantly even in the presence of high concentrations of the LPFFD peptide. The orientation direction of Aβ25-35 fibrils was not affected by LPFFD (Figures 2a and b), indicating that the interaction between Aβ25-35 peptides and the mica surface, which are the primary determinants of the oriented arrangement, are not influenced by the presence of the LPFFD peptide. The global structure of the fibrils, assessed

by the mean fibril height, was also unaffected by the LPFFD treatment (Figure 2c and d). The assembly of Aβ25-35 fibrils on mica proceeded with similar kinetics regardless of whether the LPFFD peptide was present or not (Figure 3). The observation suggests that LPFFD peptide does not significantly interfere with the binding of Aβ25-35 peptides along the axis of the fibril. As a result, high concentrations of the LPFFD peptide did not have significant effect on the global structure of an already formed, mature network of Aβ25-35 fibrils (Figure 4). The only finding that suggests a modulatory effect of LPFFD on Aβ25-35 properties was seen in nanomechanical experiments (Figure 5). In the presence of LPFFD longer force plateaus were observed with fewer force steps. Force plateaus in nanomechanical traces of amyloid fibrils are attributed to the unzipping of protofilaments from the fibril (Karsai *et al*., 2005, 2006a; Kellermayer *et al*., 2005). The height of the plateaus is related to the force necessary to unzip the protofilaments. Therefore, plateau forces are related to the mechanical stability of the fibril. The observation that the average plateau forces decreased in the presence of LPFFD suggest that the peptide may weaken the interaction between protofilaments. The length of the force plateau corresponds to the distance between consecutive protofilament rupture events. The longer the plateau, the longer it takes for the protofilament to rupture, along its length or at its attachment points, during mechanical unzipping. We can only speculate about the reasons of increased plateau length observed in the presence of LPFFD. Conceivably, the decrease in inter-protofilament interaction strength was coupled with an increase in the axial stability of the protofilament. However, more detailed experimentation will be necessary to unravel the exact mechanisms behind the finding.

Our results indicate that the LPFFD peptide does not have a significant beta-sheet-breaking effect in the amyloid assembly system utilized in the present experiments. The lack of a marked inhibitory effect of the LPFFD peptide on the structure and dynamics of the oriented network of Aβ25-35 fibrils can be attributed most likely to the sequence mismatch between the LPFFD and Aβ25-35 peptides. Although the LPFFD peptide may have a generalized beta-sheet-breaking property, it is likely that the strong interactions between the mica surface and the Aβ25-35 peptide outcompeted any minor effects. The oriented Aβ25-35 fibril network nevertheless continues to serve as a model system for more specific physical and chemical factors that may interfere with amyloid fibrillogenesis. The multiple parameters extracted in our experiments using scanning force microscopy underline the utility of this experimental model system.

CONCLUSIONS

The effect of the BSB peptide LPFFD was investigated in an amyloid model system of oriented Aβ25-35 fibrils on mica. The addition of LPFFD did not significantly alter the orientation and assembly kinetics of Aβ25-35 fibrils. Already formed fibrils did not disassemble in the presence of high concentrations of LPFFD. The mechanical stability of the fibrils was only slightly decreased, suggesting that LPFFD may moderately weaken inter-protofilament interactions. Complete disassembly of fibrils, however, was not observed. Thus, under the conditions explored here, LPFFD may not be considered as a BSB peptide with generalized beta-sheet breaking properties.

Acknowledgements

This work was supported by grants from the Hungarian Science Foundation (OTKA K73256), the Hungarian National Office of Research and Technology (NANOAMI KFKT-1-2006-0021, OMFB-380/2006), and the Hungarian Medical Research Council (ETT-229/09).

REFERENCES

Estrada LD, Soto C. 2007. Disrupting beta-amyloid aggregation for Alzheimer disease treatment. *Curr. Top. Med. Chem.* **7**(1): 115–126.

Forloni G, Chiesa R, Smiroldo S, Verga L, Salmona M, Tagliavini F, Angeretti N. 1993. Apoptosis mediated neurotoxicity induced by chronic application of beta amyloid fragment 25-35. *Neuroreport* **4**(5): 523–526.

Hardy J, Selkoe DJ. 2002. The amyloid hypothesis of Alzheimer's disease: progress and problems on the road to therapeutics. *Science (New York, NY)* **297**(5580): 353–356.

Hutter JL, Bechhoefer J. 1993. Calibration of atomic-force microscope tips. *Rev. Sci. Instrum.* **64**(7): 1868–1873.

Karsai Á, Grama L, Murvai Ü, Soós K, Penke B, Kellermayer MSZ. 2007. Potassium-dependent oriented growth of amyloid β 25-35 fibrils on mica. *Nanotechnology* **18**: 345102.

Karsai A, Martonfalvi Z, Nagy A, Grama L, Penke B, Kellermayer MS. 2006a. Mechanical manipulation of Alzheimer's amyloid beta1-4 fibrils. *J. Struct. Biol.* **155**(2): 316–326.

Karsai Á, Mártonfalvi Z, Nagy A, Grama L, Penke B, Kellermayer MSZ. 2006b. Mechanical manipulation of Alzheimer's amyloid β1-4 fibrils. *J. Struct. Biol.* **155**: 316–326.

Karsai A, Murvai U, Soos K, Penke B, Kellermayer MS. 2008. Oriented epitaxial growth of amyloid fibrils of the N27C mutant beta25-3 peptide. *Eur. Biophys. J.* **37**(7): 1133–1137.

Karsai A, Nagy A, Kengyel A, Martonfalvi Z, Grama L, Penke B, Kellermayer MS. 2005. Effect of lysine-28 side-chain acetylation on the nanomechanical behavior of alzheimer amyloid beta25-3 fibrils. *J. Chem. Inf. Model.* **45**(6): 1641–1646.

Kellermayer MS, Grama L, Karsai A, Nagy A, Kahn A, Datki ZL, Penke B. 2005. Reversible mechanical unzipping of amyloid beta-fibrils. *J. Biol. Chem.* **280**(9): 8464–8470.

Kellermayer MS, Karsai A, Benke M, Soos K, Penke B. 2008. Stepwise dynamics of epitaxially growing single amyloid fibrils. *Proc Natl Acad Sci USA* **105**(1): 141–144.

Selkoe DJ. 2001. Alzheimer's disease: genes, proteins, and therapy. *Physiol. Rev.* **81**(2): 741–766.

Selkoe DJ. 1997. Images in neuroscience. Alzheimer's disease: from genes to pathogenesis. *Am. J. Psychiatry* **154**(9): 1198.

Serpell LC, Blake CC, Fraser PE. 2000. Molecular structure of a fibrillar Alzheimer's A beta fragment. *Biochemistry* **39**(43): 13269–13275.

Sigurdsson EM, Permanne B, Soto C, Wisniewski T, Frangione B. 2000. *In vivo* reversal of amyloid-beta lesions in rat brain. *J. Neuropathol. Exp. Neurol.* **59**(1): 11–17.

Smith PK, Krohn RI, Hermanson GT, Mallia AK, Gartner FH, Provenzano MD, Fujimoto EK, Goeke NM, Olson BJ, Klenk DC. 1985. Measurement of protein using bicinchoninic acid. *Anal. Biochem.* **150**(1): 76–85.

Soto C, Sigurdsson EM, Morelli L, Kumar RA, Castano EM, Frangione B. 1998. Beta-sheet breaker peptides inhibit fibrillogenesis in a rat brain model of amyloidosis: implications for Alzheimer's therapy. *Nat. Med.* **4**(7): 822–826.

Tjernberg LO, Naslund J, Lindquist F, Johansson J, Karsltrom AL, Thyberg J, Terenius L, Nordstedt C. 1996. Arrest of β-amyloid fibril formation by a pentapeptide ligand. *J. Biol. Chem.* **271**: 8545–8548.

Tjernberg LO, Pramanik A, Björling S, Thyberg P, Thyberg J, Nordstedt C, Berndt KD, Terenius L, Rigler R. 1999. Amyloid β-peptide polymerization studied using fluorescence correlation spectroscopy. *Chem. Biol.* **6**: 53–62.

Tycko R. 2004. Progress towards a molecular-level understanding of amyloid fibrils. *Curr. Opin. Struct. Biol.* **14**: 96–103.

Yankner BA, Duffy LK, Kirschner DA. 1990. Neurotrophic and neurotoxic effects of amyloid beta protein: reversal by tachykinin neuropeptides. *Science (New York, NY)* **250**(4978): 279–282.

Zarandi M, Soos K, Fulop L, Bozso Z, Datki Z, Toth GK, Penke B. 2007. Synthesis of Abeta[1-42] and its derivatives with improved efficiency. *J. Pept. Sci.* **13**(2): 94–99.